Superthreshold Behavior and Threshold Estimates of Ultrasound-Induced Lung Hemorrhage in Adult Rats: Role of Beamwidth

William D. O'Brien, Jr., *Fellow, IEEE*, Douglas G. Simpson,
Leon A. Frizzell, *Senior Member, IEEE*, and James F. Zachary

***Abstract*—It is well documented that ultrasound-induced lung hemorrhage can occur in mice, rats, rabbits, pigs, and monkeys. The objective of this study was to assess the role of the ultrasound beamwidth (beam diameter incident on the lung surface) on lesion threshold and size. A total of 144 rats were randomly exposed to pulsed ultrasound at three exposure levels and four beamwidths (12 rats per group). The three in situ peak rarefactional pressures were about 5, 7.5, and 10 MPa. The four 19-mm-diameter focused transducers had measured pulse-echo –6-dB focal beamwidths of 470 μm (2.8 MHz; f/1), 930 μm (2.8 MHz; f/2), 310 μm (5.6 MHz; f/1), and 510 μm (5.6 MHz; f/2). Exposure durations were 10 s, pulse repetition frequencies were 1 kHz, and pulse durations were 1.3 μs (2.8 MHz; f/1), 1.2 μs (2.8 MHz; f/2), 0.8 μs (5.6 MHz; f/1) and 1.1 μs (5.6 MHz; f/2). The lesion surface area and depth were measured for each rat as well as the percentage of rats with lesions per group. Logistic regression analysis and Gaussian-Tobit analysis methods were used to analyze the data. The effects of in situ peak rarefactional pressure and beamwidth were highly significant, but ultrasonic frequency was not significant. In addition, the estimated interaction between in situ peak rarefactional pressure and beamwidth was positive and highly significant. The ultrasound beamwidth incident on the lung surface was shown to strongly affect the percentage and size of ultrasound-induced lung hemorrhage lesions. Even though ultrasonic frequency was an experimental variable, it was not shown to affect the lesion percentage or size.**

I. Introduction

The clinical use of diagnostic ultrasound continues to have a remarkable safety record in human medicine. Over the past decade, however, concerns for its safety have been raised based on experimental findings documenting lung hemorrhage in mice, rats, rabbits, monkeys and pigs [1]–[20]. In these studies, there was not a thorough evaluation of the influence of beamwidth on ultrasound-induced lung hemorrhage, although beamwidth is a major ultrasound exposure variable of diagnostic ultrasound systems. In one of these studies, however, little difference was shown in the reported thresholds of ultrasound-induced lung hemorrhage between focused and unfocused fields [1]. Beamwidth is an important variable for influencing ultrasound-induced heating [21], [22], although several studies have indicated that heating is not responsible for ultrasound-induced lung hemorrhage [1], [2], [23]. Our study reports the results of a comprehensive evaluation of the influence of beamwidth in producing ultrasound-induced lung hemorrhage in rats. Two ultrasonic frequencies (2.6 and 5.6 MHz) were used, with two beamwidths for each frequency. A previous study showed that the occurrence of ultrasound-induced lung hemorrhage was independent of these frequencies in both mice and rats [19].

Manuscript received February 7, 2001; accepted June 27, 2001. This work was supported by NIH Grant HL58218, awarded to W. D. O'Brien, Jr. and J. F. Zachary and NSF Grant DMS-0073044 awarded to D. G. Simpson.

W. D. O'Brien, Jr. and L. A. Frizzell are with the Bioacoustics Research Laboratory, Department of Electrical and Computer Engineering, University of Illinois, Urbana, IL 61801 (e-mail: wdo@uiuc.edu).

D. G. Simpson is with the Department of Statistics, University of Illinois, Champaign, IL 61820.

J. F. Zachary is with the Department of Veterinary Pathobiology, University of Illinois, Urbana, IL 61802.

TABLE I
Water-Based Pulse-Echo Ultrasonic Field Distribution Results for the Four 19-mm-Diameter Lithium Niobate Ultrasonic Transducers Tabluated by Nominal f-Number.

Pulse-echo quantity	f/1	f/2	f/1	f/2
Center frequency (MHz)	2.8	2.8	5.6	5.6
Fractional bandwidth (%)	12	11	15	13
Focal length (mm)	19	39	19	38
–6-dB focal beamwidth (μm)	470	930	310	510
–6-dB depth of focus (mm)	2.7	12	2.1	6.9

II. Materials and Methods

A. Exposimetry

Ultrasonic exposures were conducted using four focused, 19-mm-diameter, lithium niobate ultrasonic transducers (Valpey Fisher, Hopkinton, MA). Water-based (degassed water, 22°C) pulse-echo ultrasonic field distribution measurements were performed according to established procedures [19], [24] (Table I).

An automated procedure based on established standards [27], [28] was used to routinely calibrate the ultrasound fields [19], [25], [26]. Briefly, the source transducer's drive voltage was supplied by a RAM5000 (Ritec, Inc., Warwick, RI) that had the capability to deliver up to a 5-kW single-cycle pulse into a 50-Ω load (Fig. 1).

A calibrated PVDF membrane hydrophone (Marconi Model Y-34-6543, Chelmsford, UK) was mounted to

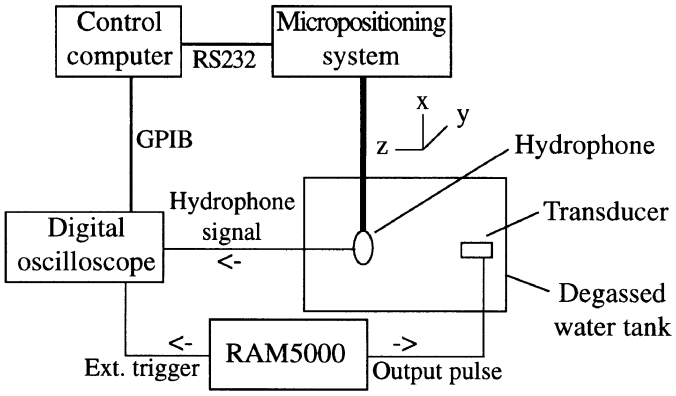

Fig. 1. Block diagram of ultrasound calibration procedure.

the computer-controlled micropositioning system (Daedal, Inc., Harrisburg, PA). The hydrophone's signal was digitized with an oscilloscope (500 Ms/s; LeCroy Model 9354TM, Chestnut Ridge, NY), the output of which was fed to the same computer (Dell Pentium II; Dell Corporation, Round Rock, TX) that controlled the positioning system. Off-line processing (Matlab; The Mathworks, Natick, MA) yielded the peak water-based rarefactional pressure $p_{r(\text{in vitro})}$ and the peak water-based compressional pressure $p_{c(\text{in vitro})}$ (Table II). The Mechanical Index (MI) was also determined [27]. The MI is reported because it is a regulated quantity [29], [30] of diagnostic ultrasound systems, and its value is available to system operators. Thus, there is value to provide the MI for each of our exposure settings, in order to give general guidance to manufacturers and operators as to the levels we are using in this study. Further, it is a quantity that cannot be determined from $p_{r(\text{in vivo})}$.

Independent calibrations were performed weekly on all four transducers during the duration of the experiment. One set of calibrations was performed before exposures were initiated each week, and one set of calibrations was performed after exposures were concluded for each week. Relative standard deviations ($\frac{\text{standard deviation}}{\text{mean}}$) of $p_{r(\text{in vitro})}$ and $p_{c(\text{in vitro})}$ were 12 and 15%, respectively, for each of the transducers. The pulse durations were also measured [28] at every calibration for each transducer, and their mean values were 1.3 μs (2.8 MHz; f/1); 1.2 μs (2.8 MHz; f/2); 0.8 μs (5.6 MHz; f/1); and 1.1 μs (5.6 MHz; f/2).

The in situ (at the pleural surface) peak rarefactional and compressional pressures were estimated from their respective in vitro peak acoustic pressures, the mean attenuation coefficient of the chest wall's intercostal tissue (2.8 dB/cm at 2.8 MHz; 5.9 dB/cm at 5.6 MHz) [31], and the mean chest wall thickness (156 rats: 3.66 ± 0.28 mm). The experimental findings were analyzed and reported in terms of the in situ peak rarefactional pressure $p_{r(\text{in situ})}$ (Table II).

B. Animals

The experimental protocol was approved by the campus' Laboratory Animal Care Advisory Committee and satisfied all campus and National Institutes of Health rules for the humane use of laboratory animals. Animals were housed in an AAALAC-approved animal facility, placed in groups of three or four in polycarbonate cages with beta-chip bedding and wire bar lids, and provided food and water ad libitum.

A total of 144 10-to-11-wk-old 257 ± 21-g female Sprague-Dawley rats (Harlan, Indianapolis, IN) were assigned to one of four beamwidth groups at random (Table I). An additional 12 rats were assigned as shams (3 per group) and incorporated into the randomized design. Three $p_{r(\text{in situ})}$ levels were estimated from the results of a previous study [19] to allow essentially the same three $p_{r(\text{in situ})}$ levels for each of the four beamwidth groups (Table II). The individuals involved in animal handling, exposure, and lesion scoring were blinded to the exposure condition. The exposure condition for each animal was revealed only after the final results were tabulated.

Rats were weighed and then anesthetized with ketamine hydrochloride (87.0 mg/kg) and xylazine (13.0 mg/kg) administered intraperitoneally. The skin of the left thorax was exposed by removing the hair with an electric clipper, followed by a depilatory agent (Nair®; Carter-Wallace, Inc., New York, NY) to maximize sound transmission. A black dot was placed on the skin over the ribs at approximately the sixth to ninth rib to guide the positioning of the ultrasonic beam. Anesthetized animals were placed in a specially designed holder to which the ultrasonic transducer was attached. A removable pointer, attached to the transducer, was used to position the ultrasonic beam, perpendicular to the skin, at the position of the black dot, with the beam's focal region approximately at the lung surface [19]. The ultrasonic beam was incident on the lateral surface of the lung.

The holder with the animal and mounted transducer was placed in degassed, temperature-controlled (30°C) water. The low-power, pulse-echo capability of the exposure system (RAM5000; Ritec, Inc., Warwick, RI) displayed on an oscilloscope was used to adjust the axial center of the focal region to within 1 mm of the lung surface. It was during this part of the experimental procedure that the 13-Ω in-line attenuator was placed between the RAM5000 and transducer to obtain very low exposure values (see sham in Table II for these low-level ultrasonic pressure levels). Also, the pulse repetition frequency was reduced to 10 Hz during this alignment procedure. The ultrasound propagation medium between the transducer and the animal's skin surface was degassed water, as was used for transducer calibrations. Animals were exposed to pulsed ultrasound with a pulse repetition frequency of 1 kHz and an exposure duration of 10 s. The 10-s exposure duration was used to simulate incidental exposure to lung tissue because, in clinical practice, the lung is generally not intentionally exposed to diagnostic ultrasound. Following exposure, rats

TABLE II
MEAN VALUES OF THE IN SITU (AT THE PLEURAL SURFACE) PEAK RAREFACTIONAL PRESSURE $p_{r(\text{IN SITU})}$ AND PEAK COMPRESSIONAL PRESSURE $p_{c(\text{IN SITU})}$.

Number of animals	$p_{r(\text{in situ})}$ (MPa)	$p_{c(\text{in situ})}$ (MPa)	MI	Lesions (%)	Mean (SEM) lesion area (mm^2)	Mean (SEM) lesion depth (mm)
Beamwidth = 470 μm; frequency = 2.8 MHz						
3 (sham)	0.26	0.28	0.15	0	—	—
12	5.11	5.07	2.57	17 (11)	2.08 (1.92)	0.22 (0.15)
12	7.61	9.39	3.90	42 (14)	1.65 (0.72)	0.54 (0.20)
12	10.2	14.3	5.26	67 (14)	2.40 (0.76)	0.85 (0.25)
Beamwidth = 930 μm; frequency = 2.8 MHz						
3 (sham)	0.26	0.28	0.15	0	—	—
12	4.93	11.8	2.16	25 (13)	0.95 (0.52)	0.28 (0.15)
12	7.53	19.9	3.27	75 (13)	5.19 (1.45)	1.25 (0.29)
12	10.2	28.1	4.40	100 (0)	16.0 (1.73)	2.72 (0.26)
Beamwidth = 310 μm; frequency = 5.6 MHz						
3 (sham)	0.23	0.26	0.063	0	—	—
12	5.04	7.49	1.74	8 (8)	0.04 (0.04)	0.02 (0.02)
12	7.57	12.1	2.55	17 (11)	0.53 (0.42)	0.26 (0.16)
12	10.1	16.8	3.38	33 (14)	1.90 (1.10)	0.36 (0.15)
Beamwidth = 510 μm; frequency = 5.6 MHz						
3 (sham)	0.23	0.26	0.063	0	—	—
12	5.46	9.88	1.36	8 (8)	0.05 (0.05)	0.06 (0.06)
12	8.04	14.9	1.99	67 (14)	2.43 (0.79)	1.04 (0.30)
12	10.7	20.1	2.64	92 (8)	7.07 (1.27)	1.93 (0.22)

All rats were exposed to pulsed ultrasound (pulse repetition frequency of 1 kHz and exposure duration of 10 s). The sham exposure conditions used a pulse repetition frequency of 10 Hz. Mean values of the MI, as measured according to the applicable standard [27], are provided because the MI is a regulated quantity of diagnostic ultrasound equipment.

were removed from the water and holder and euthanized under anesthesia by cervical dislocation.

The left thoracic wall was opened, and the thickness of the intercostal tissue (skin, fat, fascia, muscle, and parietal pleura) between the ribs was measured with a digital micrometer (accuracy: 10 μm) at the black dot used for transducer alignment. These chest wall measurements were used for later calculation of the in situ ultrasonic pressures at the visceral pleural surface. The lungs were removed from each animal, and the left lung was scored for the presence or absence of hemorrhage. As previously reported [17], [19], lung hemorrhage formed along the pathway of the ultrasound beam and the lesion assumed a conical shape. The base of the lesion originated at the visceral pleural surface and was elliptical in shape. The lesion extended into lung parenchyma to form its apex at varied depths within the lung. The left lung was fixed by immersion in 10% neutral-buffered formalin for a minimum of 24 h. After fixation, the elliptical dimensions of each lung lesion at the visceral pleural surface were measured using a digital micrometer where a is the semi-major axis and b is the semi-minor axis. The lesion was then bisected, and the depth d of the lesion within the pulmonary parenchyma was also measured. The surface area (πab) and volume ($\pi abd/3$) of the lesion were calculated for each animal. Each half of the bisected lesion was embedded in paraffin, sectioned at 5 μm, stained with hematoxylin and eosin, and evaluated microscopically.

C. Statistics

Logistic regression analysis was used to examine the dependence of the lesion incidence rates on ultrasonic frequency, in situ peak rarefactional pressure, and beamwidth. The logistic regression analysis models the log-odds of an event (i.e., occurrence of a lesion) as a linear function, with coefficients for each of the variables in the study [32]. Maximum likelihood estimates of the model parameters, estimated covariance matrices, and confidence intervals were computed using S-Plus®(Insightful Corp., Seattle, WA). Variables were selected by backward elimination. Initially, all experimental variables and their pairwise interactions were considered as candidates for inclusion in the logistic regression model. Parameters failing to achieve statistical significance in the multiple logistic regression model were eliminated from the model. Logistic regression estimates and confidence intervals were transformed to yield estimates and confidence intervals for two "effective dose" (ED) thresholds, the ED05 and ED50 thresholds (i.e., the in situ peak rarefactional pressure associated with 5 and 50% probabilities of lesions, respectively) [33]. It is understood that in situ peak rarefactional pressure is a dose in the generalized sense of an exposure quantity rather than in the specific sense of a chemical concentration.

Depth and root surface area ($\sqrt{\text{surface area}}$) of lesions were analyzed using Gaussian-Tobit regression using the

S-Plus `survReg` function. The Tobit regression model is a hybrid between a quantal threshold regression model for the occurrence of observations equal to zero and a linear regression model for observations greater than zero. Zero values are treated as the outcome of a continuous latent variable ("stress") that produces no observable outcome below a threshold. Above the threshold, the "stress" is measurable and modeled as a continuous outcome. The threshold estimate is determined by the median regression line, which is estimated from the trend of the observed continuous outcomes and the percentages of zeros. Statistically, the Tobit regression model is a censored regression model that treats zeros as continuous measurements truncated at zero [34], [35]. Parameters in the model were determined using backwards selection as described in the section on logistic regression. Initially, all variables and their pairwise interactions were considered as candidates. Parameters failing to achieve significance were eliminated. Frequency and beamwidth were forced into the model because they were primary variables to be assessed.

For animals with lesions, the depth or root surface area was included as the response measurement. For animals without lesions, the depth or root surface area was included as a zero value. Graphs of ordered residuals versus normal percentiles indicated the need for a square root transformation of surface area, in order to achieve an adequate fit of a linear Tobit model. For the Tobit model, the median lesion size (depth or root surface area) was zero up to some nonnegative value of in situ peak rarefactional pressure. Above that level, the zero crossing, the median lesion size increases linearly. The Gaussian-Tobit model allows estimation of percentiles of lesion depth or surface area as well as incidence rates for lesions. In addition to a regression line for the median response above zero, the Tobit regression provides a model for the probability of a zero measurement as a function of the regression variables. The ED05 and ED50 (in situ peak rarefactional pressure associated with a 5 and 50% incidence rate) were computed, as were the exposure levels where the probabilities of zero were 95 and 50%, respectively (incidence estimates of 5 and 50%). Standard errors were derived by first-order Taylor approximation.

III. Results

A. Percentage of Animals with Lesions

The logistic regression model for incidence of lesions [Fig. 2(a)] was highly statistically significant, with a log-likelihood ratio chi-square of 63.07 on 3 degrees of freedom and $P < 0.0001$, indicating that the association between lesions and the variables in the model cannot be explained by chance alone. Beamwidth and in situ peak rarefactional pressure were found to be significant variables. Moreover, these variables exhibit a synergism: higher in situ peak rarefactional pressure is associated with a larger effect caused by beamwidth. Frequency was not found to be a

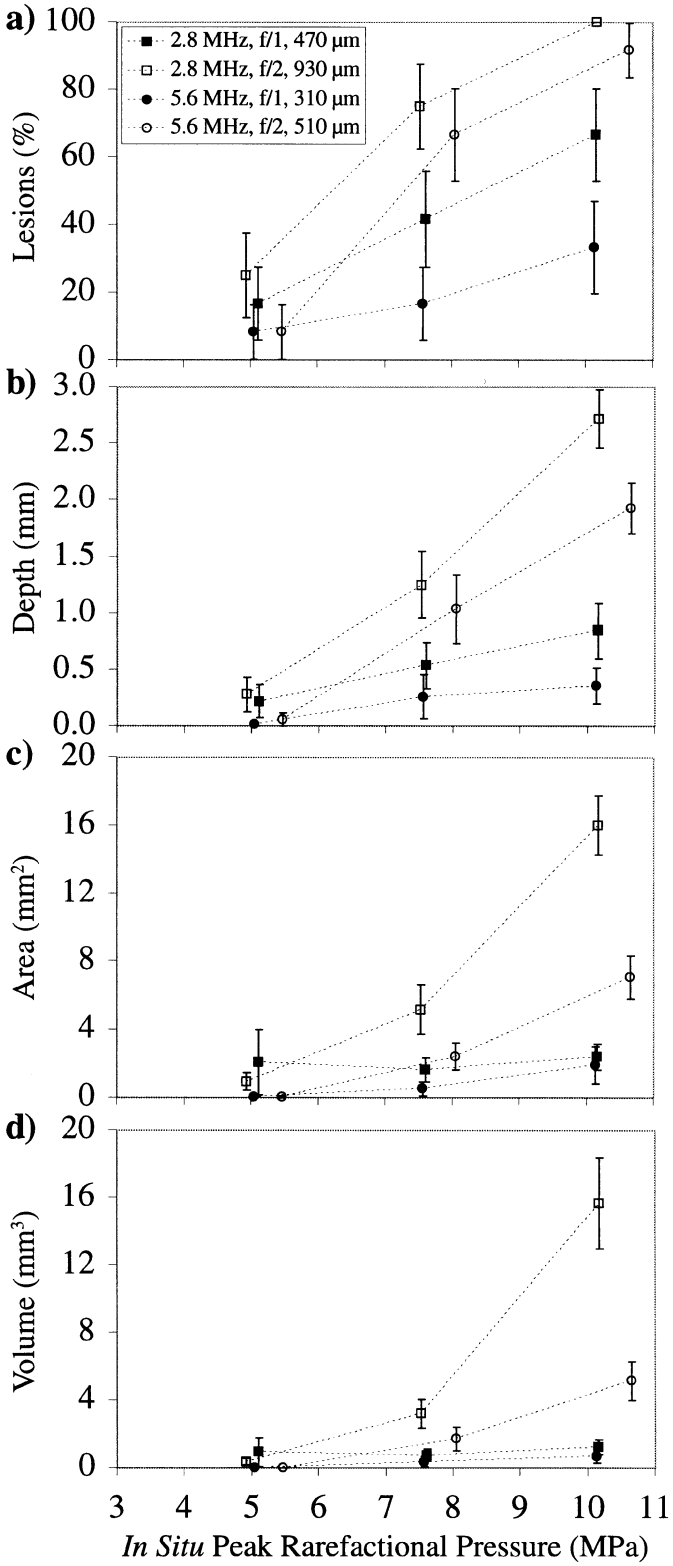

Fig. 2. a) Lesion occurrence, b) lesion depth, c) lesion surface area, and d) lesion volume as a function of the in situ peak rarefactional pressure. The dashed lines are straight lines connecting the mean values and are intended to provide graphical guidance for the four frequency/beamwidth exposures. Error bars are the standard errors of the mean (n = 12 for each exposure condition).

significant factor; however, it was included in the model for estimation purposes.

Let p denote the probability of a lesion. The estimated logistic regression model was given by

$$\log\left\{\frac{p}{1-p}\right\} = -\underbrace{3.20}_{(1.34)} + \underbrace{0.048 \cdot f}_{(0.183)} - \underbrace{0.00424 \cdot b}_{(0.00165)} + \underbrace{0.00125 \cdot b \cdot p_{r(\text{in situ})}}_{(0.00022)} \quad (1)$$

where f denotes the frequency in MHz, b denotes the beamwidth in μm, and $p_{r(\text{in situ})}$ denotes the in situ peak rarefactional pressure in MPa. Standard errors are given in parentheses. Parameter estimates in (1) may be interpreted as log-odds ratios associated with increases of one unit in the respective regression variables. Because of the interaction term in the model, the estimated effect of beamwidth depends on the acoustic pressure $p_{r(\text{in situ})}$. For example, if $p_{r(\text{in situ})} = 4.5$ MPa, then according to the model, each 1-μm increase in beamwidth increases the log-odds of a lesion by $-0.00424 + 0.00125 \cdot 4.5 = 0.001385$. Therefore, at 4.5 MPa, increasing the beamwidth from 310 to 930 μm (an increase of 620 μm) increases the estimated odds of a lesion by a factor of $e^{(620)(0.001385)} = 2.36$. Frequency ($f$) is not significant but is retained in the model for estimation purposes. The beamwidth by $p_{r(\text{in situ})}$ product in the model is a function of the energy. Technically, if the acoustic pressure is zero, then the beamwidth and frequency are zero as well. The model is not designed to extrapolate to these extreme situations. It is meant to be reliable within the range of exposures in the experiment.

The ED05 and ED50 thresholds for occurrence of lesions were obtained by setting $p = 0.05$ and 0.50 in (1) and solving for $p_{r(\text{in situ})}$. Standard errors were computed by Taylor series expansion of the resultant expression. The estimated ED05s, ED50s, and standard errors are given in Table III. The ED05 thresholds are within sampling variation of each other. This reflects the lack of a beamwidth effect at low levels of $p_{r(\text{in situ})}$. The ED50s that occur at higher acoustic pressure levels show a marked effect of beamwidth. Beamwidths of 470 μm (2.8 MHz; f/1) and 510 μm (5.6 MHz; f/2) led to slightly different ED50 estimates, but the differences were within sampling variation. The lack of a significant frequency effect over the range of the experiment is reflected in the similarity of results for 2.8 and 5.6 MHz.

B. Lesion Surface Area and Depth

The Gaussian-Tobit regressions of lesion surface area and lesion depth [Fig. 2(b and c)] indicated highly statistically significant associations with the experimental variables. In particular, the regression of root surface area on frequency, beamwidth, and the interaction between beamwidth and acoustic pressure produced a highly statistically significant model (likelihood ratio chi-square = 84.5 on 3 degrees of freedom; $P < 0.0001$), as did the regression of lesion depth on frequency, beamwidth, and the interaction between beamwidth and acoustic pressure (likelihood ratio chi-square = 86.5 on 3 degrees of freedom; $P < 0.0001$). These results indicate that the association between the size of the lesion and the experimental variables cannot be explained by chance alone.

The Tobit regression line for root surface area ($\sqrt{\text{surface area}}$) was given by:

$$y = -\underbrace{2.44}_{(1.10)} + \underbrace{0.038 \cdot f}_{(0.16)} - \underbrace{0.00395 \cdot b}_{(0.00142)} + \underbrace{0.00109 \cdot b \cdot p_{r(\text{in situ})}}_{(0.00014)} \quad (2a)$$

$$\log(\sigma) = 0.55\ (0.097) \quad (2b)$$

where f, b, and $p_{r(\text{in situ})}$ are as (1), σ^2 is the error variance, and standard errors are given in parentheses. If $y > 0$, then it denotes the median root surface area. If $y \leq 0$, then it denotes the 100th percentile of a normal distribution with mean zero and variance σ^2, where p is the probability of a lesion (surface area greater than zero). This quantity is the Gaussian-Tobit analog of the logit, $\log\{\frac{p}{1-p}\}$, on the left side of (1). Therefore, 2(a and b) were used to compute ED05 and ED50 thresholds (Table III). They exhibit similar patterns as the corresponding quantities for occurrence of lesions. The ED05 estimates were within sampling variation, with estimates ranging from 3.8 to 4.4 MPa and standard errors ranging from 1.0 to 1.6 MPa. The ED50 estimates show the significant effects of beamwidth and $p_{r(\text{in situ})}$, although beamwidths of 470 μm (2.8 MHz; f/1) and 510 μm (5.6 MHz; f/2) did not lead to significantly different estimates.

The Tobit regression line for lesion depth was given by

$$y = -\underbrace{2.13}_{(0.79)} + \underbrace{0.093 \cdot f}_{(0.11)} - \underbrace{0.0028 \cdot b}_{(0.0010)} + \underbrace{0.00080 \cdot b \cdot p_{r(\text{in situ})}}_{(0.00010)} \quad (3a)$$

$$\log(\sigma) = 0.22\ (0.096) \quad (3b)$$

where f, b, and $p_{r(\text{in situ})}$ are as in (1), σ^2 is the error variance, and standard errors are given in parentheses. ED05 and ED50 thresholds were calculated as described previously and are given in Table III. The ED05 estimates ranged from 1.8 to 3.3 MPa, and standard errors ranged from 1.0 to 1.6 MPa. Within the range of the experiment (excluding extrapolated values in Table III), the maximum difference between ED05 estimates was 1.5 MPa with a standard error of 0.91 MPa, so the ED05 estimates are within sampling variation. The ED50 estimates show significant effects of beamwidth and $p_{r(\text{in situ})}$, although beamwidths of 470 μm (2.8 MHz; f/1) and 510 μm (5.6 MHz; f/2) did not lead to significantly different estimates.

TABLE III
ESTIMATED IN SITU PEAK RAREFACTION PRESSURE THRESHOLDS FOR BEAMWIDTHS OF 310, 470, 510, AND 930 μM AT 2.8 AND 5.6 MHz FOR LESION OCCURRENCE, AREA, AND DEPTH.

Beamwidth (μm)	Frequency (MHz)	Measure	Threshold estimate* (MPa) ED05 (standard error)	ED50 (standard error)
310	2.8	Occurrence**	3.7 (±2.2)	11.3 (±2.1)
310	2.8	Area**	4.4 (±1.6)	10.5 (±1.8)
310	2.8	Depth**	2.8 (±1.6)	11.1 (±1.8)
470	2.8	Occurrence	3.6 (±1.5)	8.6 (±1.5)
470	2.8	Area	4.1 (±1.2)	8.2 (±1.3)
470	2.8	Depth	3.1 (±1.1)	8.5 (±1.3)
510	2.8	Occurrence**	3.6 (±1.5)	8.2 (±1.5)
510	2.8	Area**	4.1 (±1.1)	7.8 (±1.2)
510	2.8	Depth**	3.1 (±1.1)	8.1 (±1.2)
930	2.8	Occurrence	3.5 (±1.2)	6.0 (±1.2)
930	2.8	Area	3.9 (±1.0)	5.9 (±1.1)
930	2.8	Depth	3.3 (±1.0)	6.0 (±1.1)
310	5.6	Occurrence	3.5 (±1.8)	10.9 (±1.8)
310	5.6	Area	4.1 (±1.3)	10.2 (±1.5)
310	5.6	Depth	1.8 (±1.3)	10.0 (±1.5)
470	5.6	Occurrence**	3.4 (±1.5)	8.4 (±1.5)
470	5.6	Area**	3.9 (±1.1)	8.0 (±1.2)
470	5.6	Depth**	2.4 (±1.1)	7.8 (±1.2)
510	5.6	Occurrence	3.4 (±1.4)	8.0 (±1.4)
510	5.6	Area	3.9 (±1.1)	7.6 (±1.2)
510	5.6	Depth	2.4 (±1.1)	7.5 (±1.2)
930	5.6	Occurrence**	3.4 (±1.3)	5.9 (±1.3)
930	5.6	Area**	3.8 (±1.1)	5.8 (±1.2)
930	5.6	Depth**	2.9 (±1.1)	5.7 (±1.2)

*ED05: Obtained by inverting the logistic regression model for the 5% probability or the Tobit model for 95% censoring at zero. ED50: Obtained by inverting the logistic regression model for the 50% probability or the Tobit model for 50% censoring at zero.
**Extrapolated ED05 and ED50 estimates.

The results for lesion depth and surface area are qualitatively similar to the results for occurrence of lesions. All exhibit a significant beamwidth effect, including a positive interaction with acoustic pressure. None exhibit a significant effect caused by frequency. In addition to modeling the incidence rates, the threshold models (2) and (3) provide median size estimates when the incidence of lesions is greater than 50%.

Lesion volume was not evaluated statistically because it is not an independent variable, but it is provided graphically [Fig. 2(d)] for completeness.

IV. Discussion

The objective of this study was to assess the role of the ultrasound beamwidth (beam diameter incident on the lung surface) in rats. The incidence of lesions as well as lesion depth and surface area all exhibited a significant beamwidth effect. These findings are perhaps the first time that a beamwidth dependence for a mechanical bioeffect has been demonstrated. It is well known that there is a beamwidth dependence for thermal bioeffects [21], [22], and this dependency is built into the output display standard's thermal index [27]. However, there is no beamwidth dependence built into the MI [27] or into other recommended nonthermal biological effects indices [15].

Another notable finding is that ultrasonic frequency was not a significant factor over the range of the experiment (2.8 and 5.6 MHz) as assessed by lesion occurrence, lesion depth, and surface area. This is consistent with a previous study that showed that there was no dependence on ultrasonic frequency over the same frequency range [19] and provides further support for the reevaluation of the MI. The basis for the MI was intended to estimate the potential for mechanical bioeffects [27] and is given by

$$\mathrm{MI} = \frac{p_{r.3}}{\sqrt{f}}, \tag{4}$$

where $p_{r.3}$ is the water-based peak rarefactional pressure derated by 0.3 dB/cm-MHz at the location where the derated pulse intensity integral $PII_{.3}$ is a maximum and f is the ultrasonic frequency. The measurement procedure used to determine the MI reported herein was that from

the applicable standard [27] (Table II). The frequency dependence built into the MI was developed specifically to reflect the best idea as to the dependence of the likelihood for inertial cavitation on frequency under specified conditions [16], [27], [36]. These frequency-independent results, along with the previous findings that inertial cavitation is not responsible for ultrasound-induced lung hemorrhage [17], call into question the use of the MI to predict mechanical effects when the effects are not associated with an inertial cavitation mechanism.

An additional comment is appropriate about the use of the MI. The MI was introduced to gauge the likelihood of the onset of cavitation in an aqueous medium with appropriate nucleation sites [28], not intact tissue. To this extent, the onset, or threshold, is frequency dependent relative to the MI for the results reported herein, wherein the MI threshold is lower at the higher frequency. The MI is also appropriate for assessing the degree of lesion damage at superthreshold exposure conditions [16]. Further, the MI has been shown to increase as the degree of lung damage in rabbits increased [14].

Regarding the findings of frequency independence relative to $p_{r(\text{in situ})}$, the upper frequency used in this study was just over twice the lower frequency, giving a factor of 1.5 for the square root of frequency dependence in the MI. It is possible that exposures over a wider frequency range might reveal a frequency effect not observed here. Even in our previous work, we suggested a frequency dependence of lung hemorrhages in adult rabbits over the 3- to 6-MHz frequency range [14]. Further, it is interesting to observe that the ultrasonic threshold dose for production of irreversible lesions in mammalian brain was initially shown to be frequency dependent [37]. However, the lesion threshold was later shown to be frequency independent over an extended frequency range (1 to 9 MHz) when the collagenous trabeculae of the subarachnoid space, interposed between the arachnoid and the pia mater, was considered [38], [39].

The initial study design was based on the same three $p_{r(\text{in situ})}$ levels of 5.0, 7.5, and 10 MPa for each of the four transducers. To achieve these in situ exposure conditions, the calibrated in vitro exposure conditions had to take into account the rat's intercostal tissue thickness and attenuation coefficient. The intercostal tissue results from previous studies [19], [31] were used to estimate the in vitro peak rarefactional pressure levels that would yield the designed $p_{r(\text{in situ})}$ levels. Two (2.8 MHz, 470-μm beamwidth and 5.6 MHz, 510-μm beamwidth) of the four transducers used herein were those used in the previous study [19]. Following the experiments, the $p_{r(\text{in situ})}$ values used herein were slightly different from the design values, and the differences were due to the different chest wall thicknesses. The design values were based on the results from a previous study [19], wherein the lowest and highest $p_{r(\text{in situ})}$ values spanned lesion occurrence rates (percentage of lesions) from about 10 to 80%, and the middle $p_{r(\text{in situ})}$ value was about halfway between the two extreme values. With this design, there was assurance that lesion production and threshold estimation as a function of beamwidth would be evaluated properly; that is, lesion occurrence rates would be obtained within the indicated range.

The characteristics of the lesions produced in rats from this study were similar to those of mice and rats described in previous studies [3], [7], [8], [17]–[20], and, as before, these findings suggest a common pathogenesis in the initiation and propagation of the lesions as observed at the gross and microscopic levels.

At the middle and highest $p_{r(\text{in situ})}$ values (ca. 7.5 and 10 MPa), it is interesting to observe that there is an increased effect (incidence, depth, surface area, and volume) as the beamwidth is increased (Fig. 2). For the approximately same $p_{r(\text{in situ})}$ value, this would suggest that there might be an ultrasonic energy effect. To evaluate this proposition, an estimate of the energy per pulse is calculated from the product of the instantaneous power per pulse and the pulse duration. The energy per pulse is directly proportional to the delivered ultrasonic energy per exposure, because the exposure duration (10 s) and pulse repetition frequency (1 kHz) were the same for all exposures (10 000 pulses per exposure). The in situ (at the pleural surface) instantaneous pulse power is numerically calculated from

$$W_i = \int I_i(r) dS \tag{5}$$

where $I_i(r)$ is the instantaneous pulse intensity, and dS is the incremental area of the annulus as a function of r, the distance lateral from the beam axis. The lateral intensity distribution of the pulse in the focal region from a spherically focused transducer, the region that is incident on the lung surface, is assumed to be [40]

$$I_i(r) = I_0 \ \text{jinc}^2\left(\frac{r \cdot D}{2 \cdot \lambda \cdot ROC}\right), \tag{6}$$

where $I_0 = p^2_{r(\text{in situ})}/\rho c$ is the instantaneous on-axis intensity based on $p_{r(\text{in situ})}$, the in situ peak rarefactional pressure; $\rho c = 1.5$ Mrayl, the medium's specific acoustic impedance for a plane wave; $\text{jinc}(X) = J_1(2\pi X)/\pi X$, where $J_1(\cdot)$ is the Bessel function of the first kind of order one; D is the source diameter; λ is the acoustic wavelength in the propagation medium; and ROC is the source's radius of curvature, which for this calculation is assumed to be the source's measured focal length (Table I). The numerical limits of integration included the lateral distribution from the beam axis to the first zero of the jinc function. If the outer limit of integration were the –3-dB transmit beamwidth (the –6-dB pulse-echo focal beamwidth listed in Table I), then the in situ instantaneous pulse powers would have been about 57% of those values. The in situ energy per pulse is calculated from the product of the in situ instantaneous power per pulse and the pulse duration. Thus, the temporal waveform for the instantaneous intensity is taken to be rectangular, with height I_0 and a duration equal to the respective pulse durations. The temporal waveform for the instantaneous power is then rectangular as well.

The general trends of the effects (incidence, depth, surface area, and volume) as a function of the in situ energy per pulse (Fig. 3) suggests a dependence on the incident ultrasonic energy. Indeed, the logistic and Tobit regression models in (1), 2(a), and 3(a) all included the term $b \cdot p_{r(\text{in situ})}$, the square root of the ultrasonic energy, and it was highly statistically significant in each case. These observations suggest that the ultrasonic energy might be considered in future study designs and possibly in considering the basis for the MI. This suggestion, however, is tentative until an independent experiment verifies this observation, that is, until a wider range of pulse durations is a major experimental variable.

Two of the same transducers used in this study (2.8 MHz, 470-μm beamwidth and 5.6 MHz, 510-μm beamwidth) were used in a previous study [19]. Further, both studies used rats, although the study designs were different. In any case, because there is a database against which two transducer exposure groups can be compared, the in situ energy per pulse was calculated for the previous study, and the results are graphically shown in Fig. 4. It is encouraging that there is general agreement between the two studies.

The study design was not as extensive in terms of providing solid threshold estimates as our previous study [19]. In that study, at least seven $p_{r(\text{in situ})}$ levels were used to estimate the ultrasonic-induced lung hemorrhage ED05 thresholds for occurrence (lesion percentage). Nevertheless, even with three levels of $p_{r(\text{in situ})}$ used in this study, there is value in estimating the ED05 for comparison purposes. The ED05 occurrence thresholds at 2.8 and 5.6 MHz, respectively, ranged between 3.5 and 3.7 MPa, and between 3.4 and 3.5 MPa, somewhat higher than that previously observed (2.3 MPa at 2.8 MHz and 2.8 MPa at 5.6 MHz [19]). The ED05 estimates derived from root surface area regression are similar to those for occurrence. It is interesting that the ED05 estimates for depth are lower and exhibit a weak trend opposite to that previously observed (2.8 to 3.3 MPa at 2.8 MHz and 1.8 to 2.9 MPa at 5.6 MHz [19]); however, the differences are within the sampling variation indicated by the standard errors. Possibly, the lower ED05 estimates for depth indicate that this component of lesion initiation is more responsive than the surface area to lower acoustic pressure settings.

Also of note is the difference in threshold levels reported in a summary document [16] compared with those reported herein (Table III). The summary document reported lower threshold values (ca. 0.6 to 1.3 MPa) over the 1- to 4-MHz frequency range and further reported that these threshold values were dependent on frequency (derated rarefactional threshold pressure regression function of $0.63f^{0.54}$). However, the observations reported herein had higher and frequency-independent threshold values (ca. 2 to 4 MPa; Table III) over the 3- to 6-MHz frequency range. The difference in threshold values may be due to the difference in exposure durations; the summary data experiments typically used exposure durations of at least 180 s, whereas the exposure duration used herein was 10 s. The contrast

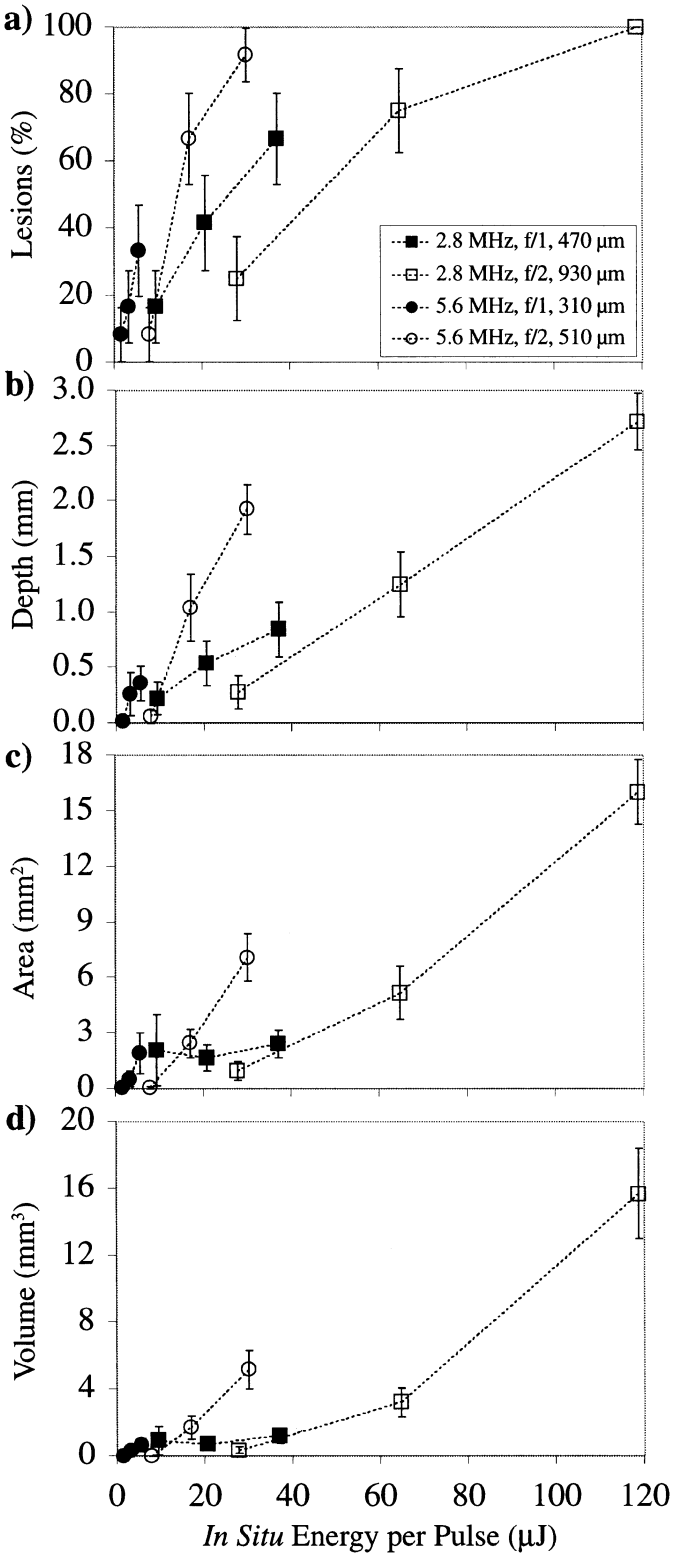

Fig. 3. (a) Lesion occurrence, (b) lesion depth, (c) lesion surface area, and (d) lesion volume as a function of the in situ energy per pulse. The dashed lines are straight lines connecting the mean values and are intended to provide graphical guidance for the four frequency/beamwidth exposures. Error bars are the standard errors of the mean (n = 12 for each exposure condition).

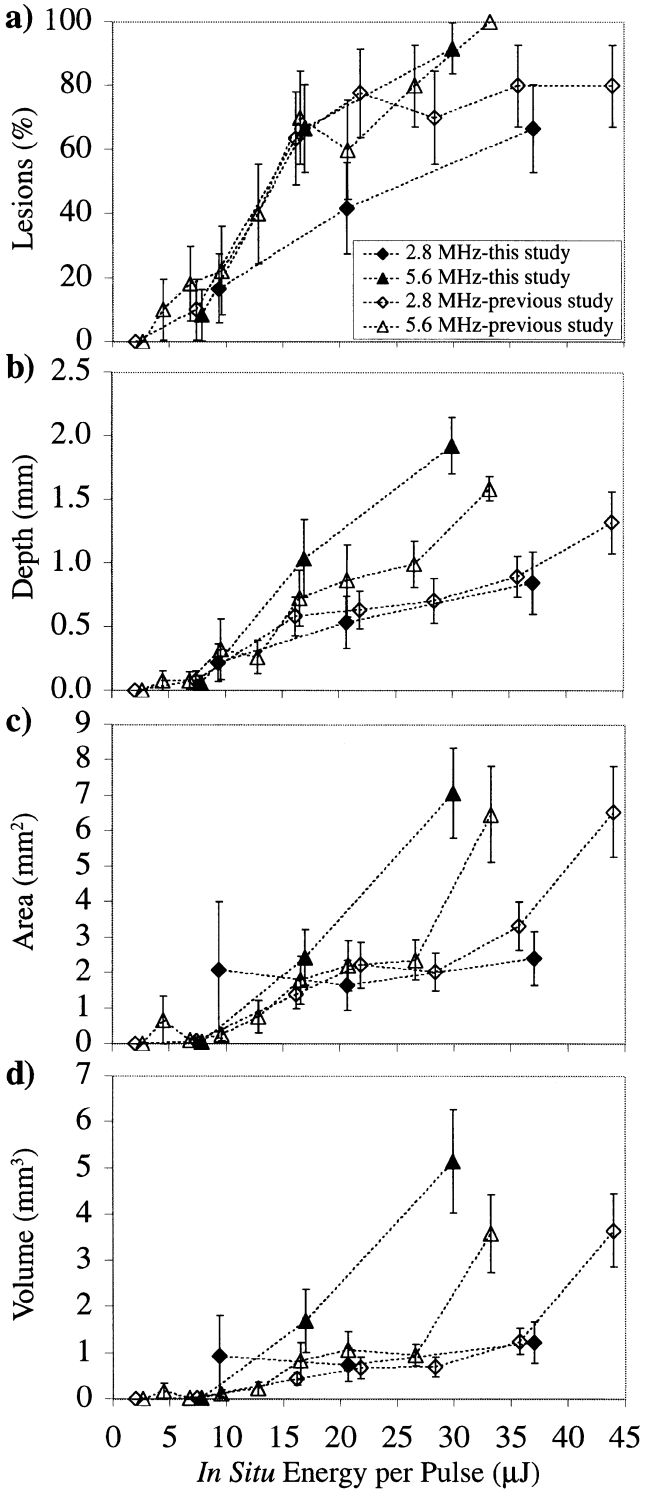

Fig. 4. Comparison of the a) lesion occurrence, b) lesion depth, c) lesion surface area, and d) lesion volume as a function of the in situ energy per pulse for the rats exposed with the same two transducers (2.8 MHz, 470-μm beamwidth and 5.6 MHz, 510-μm beamwidth) in this study and in a previous study [19]. The dashed lines are straight lines connecting the mean values and are intended to provide graphical guidance for the four frequency/beamwidth exposures. Error bars are the standard errors of the mean (n = 12 for each exposure condition in this study and n = 10 for each exposure condition in the previous study).

noted about frequency dependency may be due to the fact that the summary data were compiled from several studies using different species (mouse, rat, and pig) from different laboratories, whereas the same species was used herein with the same experimental protocol.

Acknowledgments

We thank D. Abano, J. Blue, J. Brown, T. Burns, J. Christoff, K. Clements, M. Ho, H. Luo, R. Miller, K. Norrell, and B. Zierfuss for technical contributions.

References

[1] S. Z. Child, C. L. Hartman, L. A. Schery, and E. L. Carstensen, "Lung damage from exposure to pulsed ultrasound," *Ultrasound Med. Biol.*, vol. 16, pp. 817–825, 1990.

[2] C. Hartman, S. Z. Child, R. Mayer, E. Schenk, and E. L. Carstensen, "Lung damage from exposure to the fields of an electrohydraulic lithotripter," *Ultrasound Med. Biol.*, vol. 16, pp. 675–679, 1990.

[3] D. P. Penney, E. A. Schenk, K. Maltby, C. Hartman-Raeman, S. Z. Child, and E. L. Carstensen, "Morphologic effects of pulsed ultrasound in the lung," *Ultrasound Med. Biol.*, vol. 19, pp. 127–135, 1993.

[4] C. H. Raeman, S. Z. Child, and E. L. Carstensen, "Timing of exposures in ultrasonic hemorrhage of murine lung," *Ultrasound Med. Biol.*, vol. 19, pp. 507–517, 1993.

[5] L. A. Frizzell, E. Chen, and C. Lee, "Effects of pulsed ultrasound on the mouse neonate: Hind limb paralysis and lung hemorrhage," *Ultrasound Med. Biol.*, vol. 20, pp. 53–63, 1994.

[6] C. K. Holland, K. Sandstrom, X. Zheng, J. Rodriguey, and R. A. Roy, "The acoustic field of a pulsed Doppler diagnostic ultrasound system near a pressure-release surface," *J. Acoust. Soc. Amer.*, vol. 95, p. 2855, 1994.

[7] A. F. Tarantal and D. R. Canfield, "Ultrasound-induced lung hemorrhage in the monkey," *Ultrasound Med. Biol.*, vol. 20, pp. 65–72, 1994.

[8] J. F. Zachary and W. D. O'Brien, Jr., "Lung lesion induced by continuous- and pulsed-wave (diagnostic) ultrasound in mice, rabbits, and pigs," *Vet. Pathol.*, vol. 32, pp. 43–54, 1995.

[9] R. Baggs, D. P. Penney, C. Cox, S. Z. Child, C. H. Raeman, D. Dalecki, and E. L Carstensen, "Thresholds for ultrasonically induced lung hemorrhage in neonatal swine," *Ultrasound Med. Biol.*, vol. 22, pp. 119–128, 1996.

[10] C. K. Holland, C. X. Deng, R. E. Apfel, J. L. Alderman, L. A. Ferandez, and K. J. W. Taylor, "Direct evidence of cavitation in vivo from diagnostic ultrasound," *Ultrasound Med. Biol.*, vol. 22, pp. 917–925, 1996.

[11] C. H. Raeman, S. Z. Child, D. Dalecki, C. Cox, and E. L. Carstensen, "Exposure-time dependence of the threshold for ultrasonically induced murine lung hemorrhage," *Ultrasound Med. Biol.*, vol. 22, pp. 139–141, 1996.

[12] D. Dalecki, S. Z. Child, C. H. Raeman, C. Cox, D. P. Penney, and E. L. Carstensen, "Age dependence of ultrasonically induced lung hemorrhage in mice," *Ultrasound Med. Biol.*, vol. 23, pp. 767–776, 1997.

[13] D. Dalecki, S. Z. Child, C. H. Raeman, C. Cox, and E. L. Carstensen, "Ultrasonically induced lung hemorrhage in young swine," *Ultrasound Med. Biol.*, vol. 23, pp. 777–781, 1997.

[14] W. D. O'Brien, Jr. and J. F. Zachary, "Lung damage assessment from exposure to pulsed-wave ultrasound in the rabbit, mouse, and pig," *IEEE Trans. Ultrason., Ferroelect., Freq. Contr.*, vol. 44, pp. 473–485, 1997.

[15] "WFUMB Symposium on Safety of Ultrasound in Medicine: Issues and Recommendations Regarding Non-Thermal Mechanisms for Biological Effects of Ultrasound," *Ultrasound Med. Biol.*, vol. 24, Supplement I, pp. S1–S55, 1998.

[16] American Institute of Ultrasound in Medicine, "Mechanical Bioeffects from Diagnostic Ultrasound: AIUM Consensus Statements," *J. Med. Ultrasound*, vol. 19, pp. 67–168, 2000.

[17] W. D. O'Brien, Jr., L. A. Frizzell, R. M. Weigel, and J. F. Zachary, "Ultrasound-induced lung hemorrhage is not caused by inertial cavitation," *J. Acoust. Soc. Amer.*, vol. 108, pp. 1290–1297, 2000.

[18] W. D. O'Brien, Jr., L. A. Frizzell, D. J. Schaeffer, and J. F. Zachary, "Superthreshold behavior of ultrasound induced lung hemorrhage in adult mice and rats: Role of pulse repetition frequency and pulse duration," *Ultrasound Med. Biol.*, vol. 27, pp. 267–277, 2001.

[19] J. F. Zachary, J. M. Sempsrott, L. A. Frizzell, D. G. Simpson, and W. D. O'Brien, Jr., "Superthreshold behavior and threshold estimation of ultrasound-induced lung hemorrhage in adult mice and rats," *IEEE Trans. Ultrason., Ferroelect., Freq. Contr.*, vol. 48, pp. 581–592, 2001.

[20] J. F. Zachary, L. A. Frizzell, K. S. Norrell, J. P. Blue, R. J. Miller, and W. D. O'Brien, Jr., "Temporal and spatial evaluation of lesion reparative responses following exposure of rat lung to pulsed ultrasound," *Ultrasound Med. Biol.*, vol. 27, pp. 829–839, 2001.

[21] National Council on Radiation Protection and Measurements (NCRP), Bethesda, MD, "Exposure Criteria for Medical Diagnostic Ultrasound: I. Criteria Based on Thermal Mechanisms," Report No. 113, 1992.

[22] W. D. O'Brien, Jr., and D. S. Ellis, "Evaluation of the Soft-Tissue Thermal Index," *IEEE Trans. Ultrason., Ferroelect., Freq. Contr.*, vol. 46, pp. 1459–1476, 1999.

[23] C. L. Hartman, S. Z. Child, D. P. Penney, and E. L. Carstensen, "Ultrasonic heating of lung tissue," *J. Acoust. Soc. Amer.*, vol. 91, pp. 513–516, 1992.

[24] K. Raum and W. D. O'Brien, Jr., "Pulse-echo field distribution measurement technique of high-frequency ultrasound sources," *IEEE Trans. Ultrason., Ferroelect., Freq. Contr.*, vol. 44, pp. 810–815, 1997.

[25] J. M. Sempsrott and W. D. O'Brien, Jr., "Experimental verification of acoustic saturation," in *Proc. IEEE Ultrason. Symp.*, 1999, pp. 1287–1290.

[26] J. M. Sempsrott, "Experimental evaluation of acoustic saturation," M. S. thesis, Department of Electrical and Computer Engineering, University of Illinois, Urbana, IL, 2000.

[27] *Standard for the Real-Time Display of Thermal and Mechanical Acoustic Output Indices on Diagnostic Ultrasound Equipment, Rev. 1*, Laurel, MD: American Institute of Ultrasound in Medicine, and Rosslyn, VA: National Electrical Manufacturers Association, 1998.

[28] *Acoustic Output Measurement Standard for Diagnostic Ultrasound Equipment*, Laurel, MD: American Institute of Ultrasound in Medicine, and Rosslyn, VA: National Electrical Manufacturers Association, 1998.

[29] Center for Devices and Radiological Health, US Food and Drug Administration, "Use of mechanical index in place of spatial peak, pulse average intensity in determining substantial equivalence," Rockville, MD, April 14, 1994.

[30] Center for Devices and Radiological Health, US Food and Drug Administration, "Information for manufacturers seeking marketing clearance of diagnostic ultrasound systems and transducers," Rockville, MD, September 30, 1997.

[31] G. A. Teotico, R. J. Miller, L. A. Frizzell, J. F. Zachary, and W. D. O'Brien, Jr., "Attenuation coefficient estimates of mouse and rat chest wall," *IEEE Trans. Ultrason., Ferroelect., Freq. Contr.*, vol. 48, pp. 593–601, 2001.

[32] D. W. Hosmer and S. Lemeshow, *Applied Logistic Regression*. New York: Wiley, 1989.

[33] D. G. Simpson, R. J. Carroll, H. Zhou, and D. J. Guth, "Interval censoring and marginal analysis in ordinal regression," *J. Agric., Biol., Environ. Stat.*, vol. 1, pp. 354–376, 1996.

[34] L. Billard, "Presidential invited address: The world of biometry," *Biometrics*, vol. 50, pp. 899–916, 1994.

[35] H. Galfalvy and D. G. Simpson, "Infrastructure degradation: An application of censored regression models," in *ASA Proc. Section Phys. Eng. Sci.*, pp. 242–247, 1999.

[36] C. K. Holland and R. E. Apfel, "An improved theory for the prediction of microcavitation due to pulsed ultrasound," *IEEE Trans. Ultrason., Ferroelect., Freq. Contr.*, vol. 36, pp. 204–208, 1989.

[37] F. J. Fry, G. Kossoff, R. C. Eggleton, and F. Dunn, "Threshold ultrasonic dosages for structural changes in the mammalian brain," *J. Acoust. Soc. Amer.*, vol. 48, pp. 1413–1417, 1970.

[38] R. L. Johnston and F. Dunn, "Influence of subarachnoid structures on transmeningeal ultrasonic propagation," *J. Acoust. Soc. Amer.*, vol. 60, pp. 1225–1227, 1976.

[39] R. L. Johnston, "Dose-effect relationships for ultrasound irradiation of brain tissue," Ph.D. Dissertation, University of Illinois, Urbana, IL, 1979.

[40] G. S Kino, *Acoustic Waves: Devices, Imaging, and Analog Signal Processing*. Englewood Cliffs, NJ: Prentice-Hall, Inc., p. 185.

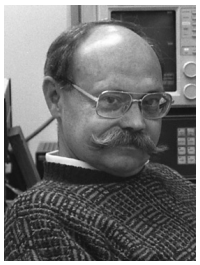

William D. O'Brien, Jr. (S'64–M'70–SM'79–F'89) received the B.S., M.S., and Ph.D. degrees in 1966, 1968, and 1970, from the University of Illinois, Urbana-Champaign.

From 1971 to 1975 he worked with the Bureau of Radiological Health (currently the Center for Devices and Radiological Health) of the U.S. Food and Drug Administration. Since 1975, he has been at the University of Illinois, where he is a Professor of Electrical and Computer Engineering and of Bioengineering, College of Engineering; Professor of Bioengineering, College of Medicine; Professor of Nutritional Sciences, College of Agricultural, Consumer and Environmental Sciences; a Research Professor in the Beckman Institute for Advanced Science and Technology; and a Research Professor in the Coordinated Science Laboratory. He is the Director of the Bioacoustics Research Laboratory and is the Program Director of the NIH Radiation Biophysics and Bioengineering in Oncology Training Program. His research interests involve the many areas of ultrasound-tissue interaction, including spectroscopy, risk assessment, biological effects, tissue characterization, dosimetry, blood-flow measurements, acoustic microscopy and imaging for which he has published 215 papers.

Dr. O'Brien is Editor-in-Chief of the *IEEE Transactions on Ultrasonics, Ferroelectrics, and Frequency Control*. He is a Fellow of the Institute of Electrical and Electronics Engineers (IEEE), the Acoustical Society of America (ASA) and the American Institute of Ultrasound in Medicine (AIUM), and a Founding Fellow of the American Institute of Medical and Biological Engineering. He was recipient of the IEEE Centennial Medal (1984), the AIUM Presidential Recognition Awards (1985 and 1992), the AIUM/WFUMB Pioneer Award (1988), the IEEE Outstanding Student Branch Counselor Award for Region 4 (1989), the AIUM Joseph H. Holmes Basic Science Pioneer Award (1993), and the IEEE Ultrasonics, Ferroelectrics, and Frequency Control Society Distinguished Lecturer (1997–1998). He received the IEEE Ultrasonics, Ferroelectrics, and Frequency Control Society's Achievement Award for 1998, and the IEEE Millennium Medal in 2000. He has served as Co-Chair of the 1981 IEEE Ultrasonic Symposium, and General Chair of the 1988 IEEE Ultrasonics Symposium, and is Co-Chair of both the 2001 and 2003 IEEE Ultrasonics Symposia. He has been Secretary-Treasurer (1972–1980), Vice President (1981), and President (1982–1983) of the IEEE Sonics and Ultrasonics Group (currently the IEEE Ultrasonics, Ferroelectrics, and Frequency Control Society). He has been Treasurer (1982–1985), President-Elect (1986–1988) and President (1988–1991) of the American Institute of Ultrasound in Medicine. He has served on the Board of Directors (1988–1993) of the American Registry of Diagnostic Medical Sonographers, and has been Treasurer (1991–1994) of the World Federation for Ultrasound in Medicine and Biology.

Douglas G. Simpson received the B.A. degree in 1980 from Carleton College and the M.S. and Ph.D. degrees in 1983 and 1985 from the University of North Carolina at Chapel Hill.

From 1985 he has been at the University of Illinois at Urbana-Champaign, where he is Professor and Chair of the Department of Statistics, former Director of the Illinois Statistics Office, and a member of the Faculty of the Interdisciplinary Environmental Toxicology Program. His research interests include computational statistics, environmental toxicology, chemometrics, generalized regression analysis, multivariate analysis and robust inference. He has published more than 35 papers.

Dr. Simpson is an Associate Editor of *Biometrics*, co-editor of *Sankhya*, a member of the editorial board of *Chemometrics and Intelligent Laboratory Systems*, and a former Associate Editor of the *Journal of the American Statistical Association*. He is a Fellow of the American Statistical Association (ASA) and the Institute of Mathematical Statistics (IMS). He has served as IMS Representative to the AMS/IMS/SIAM Joint Committee on Summer Research Conferences (1995–1997) and as a review panelist for the EPA/NSF Environmental Statistics program (2000). He was the 1997 Program Chair of the ASA Biometrics Section for the Spring Meetings of the ASA, IMS and Biometric Society, and the 1999 Program Chair for the ASA Section on Statistical Consulting.

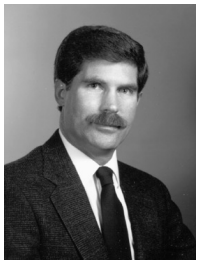

Leon A. Frizzell (S'71–M'74–SM'82) was born in West Stewartstown, NH, on September 12, 1947. He received the B.S. degree in physics from the University of New Hampshire, Durham, in 1969, and the M.S. and Ph.D. degrees in electrical engineering from the University of Rochester, Rochester, NY, in 1971 and 1976, respectively.

Since 1975, he has been in the Department of Electrical and Computer Engineering at the University of Illinois at Urbana-Champaign, where he is currently a professor of electrical and computer engineering and bioengineering. He was Acting Director of the Bioacoustics Research Laboratory within the Department of Electrical and Computer Engineering from August 1989 to August 1990 and served as Chair of the Bioengineering Faculty from August 1995 to December 1999. He was also a visiting research scientist at Yale University from August 1985 to August 1986. His research interest are in ultrasound and include tissue characterization, biological effects, hyperthermia, surgery, and bioengineering.

Dr. Frizzell is a Fellow of the American Institute of Ultrasound in Medicine, Fellow of the Acoustical Society of America, Fellow of the American Institute for Medical and Biological Engineering, and a member of Eta Kappa Nu and Sigma Xi.

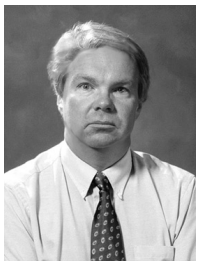

James F. Zachary received the B.S. Degree from Northern Illinois University, DeKalb in 1972 and D.V.M. and Ph.D. degrees in 1977 and 1983, respectively, from the University of Illinois, Urbana-Champaign.

From 1978, he has been at the University of Illinois, where he is a Professor of Pathology and a Bioengineering Faculty Member. His research interests involve ultrasound-tissue interaction and include biological effects, tissue characterization, bloodflow measurements, and acoustic microscopy. He has published more than 60 papers.

Dr. Zachary has served as Editor-in-Chief of *Veterinary Pathology* and is currently a co-editor of the textbook *Thomson's Special Veterinary Pathology*. He is a Diplomate of the American College of Veterinary Pathologists and a member of the American Institute of Ultrasound in Medicine (AIUM), the American Society for Investigative Pathology (ASIP-FASEB), and the Society for Neuroscience. He currently is a member of the AIUM Bioeffects Committee.